



PAPER • OPEN ACCESS

## Topological phase transitions and Majorana zero modes in DNA double helix coupled to s-wave superconductors

To cite this article: Qiao Chen *et al* 2021 *New J. Phys.* **23** 093047

View the [article online](#) for updates and enhancements.

You may also like

- [2021 Roadmap: electrocatalysts for green catalytic processes](#)  
Jiandong Liu, Jianmin Ma, Zhicheng Zhang *et al.*
- [Discovery of a New Gamma-Ray Source, LHAASO J0341+5258, with Emission up to 200 TeV](#)  
Zhen Cao, F. Aharonian, Q. An *et al.*
- [First M87 Event Horizon Telescope Results. VII. Polarization of the Ring](#)  
The Event Horizon Telescope Collaboration, Kazunori Akiyama, Juan Carlos Algaba *et al.*



## PAPER

Topological phase transitions and Majorana zero modes in DNA double helix coupled to *s*-wave superconductors

## OPEN ACCESS

RECEIVED  
9 May 2021REVISED  
25 August 2021ACCEPTED FOR PUBLICATION  
15 September 2021PUBLISHED  
30 September 2021

Original content from  
this work may be used  
under the terms of the  
[Creative Commons  
Attribution 4.0 licence](#).

Any further distribution  
of this work must  
maintain attribution to  
the author(s) and the  
title of the work, journal  
citation and DOI.

Qiao Chen<sup>1</sup> , Ai-Min Guo<sup>2,\*</sup>, Jie Liu<sup>3</sup> , F M Peeters<sup>4,5</sup> and Qing-Feng Sun<sup>6,7,8</sup><sup>1</sup> Department of Maths and Physics, Hunan Institute of Engineering, Xiangtan 411104, People's Republic of China<sup>2</sup> Hunan Key Laboratory for Super-microstructure and Ultrafast Process, School of Physics and Electronics, Central South University, Changsha 410083, People's Republic of China<sup>3</sup> Department of Applied Physics, School of Science, Xi'an Jiaotong University, Xi'an 710049, People's Republic of China<sup>4</sup> Department of Physics, University of Antwerp, Groenenborgerlaan 171, B-2020 Antwerp, Belgium<sup>5</sup> School of Physics and Astronomy and Yunnan Key Laboratory for Quantum Information, Yunnan University, Kunming 650091, People's Republic of China<sup>6</sup> International Center for Quantum Materials, School of Physics, Peking University, Beijing 100871, People's Republic of China<sup>7</sup> Collaborative Innovation Center of Quantum Matter, Beijing 100871, People's Republic of China<sup>8</sup> CAS Center for Excellence in Topological Quantum Computation, University of Chinese Academy of Sciences, Beijing 100190, People's Republic of China

\* Author to whom any correspondence should be addressed.

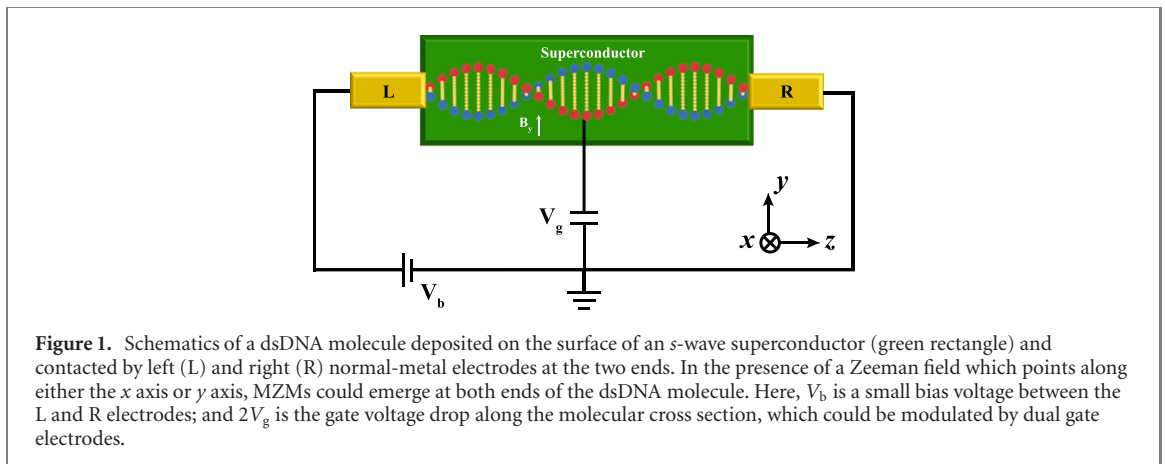
E-mail: [aimin.guo@csu.edu.cn](mailto:aimin.guo@csu.edu.cn)**Keywords:** topological phase transitions, Majorana zero modes, double-stranded DNA**Abstract**

Topological properties of a double-stranded DNA (dsDNA) proximity-coupled by an *s*-wave superconductor are investigated, in which the energy spectra and the differential conductance are calculated within the framework of tight-binding approximation. Our results indicate that this dsDNA-superconductor system hosts Majorana zero modes (MZMs) when the Zeeman field is perpendicular to the helix axis, whereas no MZM could be observed when the Zeeman field is parallel to the helix axis, in sharp contrast to previous studies on nanowires including single-stranded DNA. In particular, two topological phase transitions could take place in the dsDNA-superconductor system by changing the Zeeman field, one from a topological trivial phase to a topological nontrivial phase with one pair of MZMs in small Zeeman field regime, and the other from a phase with one pair of MZMs to a phase with two pairs of MZMs by further increasing the Zeeman field. In the presence of a gate field normal to the helix axis, the topological nontrivial phase with two pairs of MZMs can transform into the phase with one pair of MZMs. The topological phase with one pair of MZMs is more stable and robust against Anderson disorder.

**1. Introduction**

In recent years, Majorana zero modes (MZMs) have been attracting extensive and ongoing interest by the condensed matter and materials physics communities [1–14]. MZMs are quasiparticle excitations which are identical to their own antiparticles and hold great promise for implementing topological quantum computation owing to the non-Abelian exchange statistics [15–20]. Kitaev has put forward a seminal model that one-dimensional (1D) spinless *p*-wave superconducting nanowires could host MZMs at the nanowire's ends [1], which is extremely challenging experimentally as *p*-wave superconductors are rare in nature. Since the original proposal by Fu and Kane that topological insulators proximitized by *s*-wave superconductors could lead to MZMs at vortices [2], MZMs have been reported in a variety of condensed-matter systems, including 1D strong spin-orbit-coupled semiconductor-superconductor heterostructures [21–27], ferromagnetic atomic chains on superconducting substrates [28–32], planar Josephson junctions [33–38], as well as iron-based superconductors [39–43].

It has been shown that the emergence of zero-bias conductance peaks (ZBPs) in the transmission spectra is regarded as a strong signature of MZMs [3–5]. The ZBP was firstly observed in InSb semiconductor



nanowires covered by NbTiN superconductors in 2012 [24] and then reproduced in other experiments [8–11]. Besides, ZBPs were also demonstrated in atomic chains [28] and topological insulators proximitized by *s*-wave superconductors [12]. However, the value of these ZBPs is usually much smaller than conductance quantum  $2e^2/h$  and several alternative explanations beyond topological superconductivity were proposed to rationalize the ZBPs, including disorder [44, 45], weak antilocalization [46], Kondo effect [47] as well as subgap excitations [48]. Remarkably, the recent observation of quantized conductance plateau at  $2e^2/h$  at zero-bias at the center of the vortex in an iron-based superconductor is a significant breakthrough for identifying the existence of MZMs [43].

DNA, as the carrier of genetic information in biological systems, is envisioned as an important candidate for molecular electronics. On the one hand, DNA exhibits remarkable self-assembly which is key for designing unique nanodevices and delivering drugs toward cells [49–51]. These nanodevices possess the advantage of biocompatibility in comparison with other organic and inorganic materials. On the other hand, charge transport experiments have demonstrated several intriguing phenomena of double-stranded DNA (dsDNA), such as field-effect transistors [52–54] and chirality-induced spin selectivity [55–57]. In particular, as early as 2001, Kasumov *et al* have measured electron transport along double-stranded  $\lambda$ -DNA molecules bridged between two superconducting electrodes, finding that these dsDNA devices display proximity-induced superconductivity and a ZBP can be observed under moderate magnetic field [58]. Very recently, Millo *et al* have fabricated a self-assembled monolayer of chiral molecules on different superconducting substrates and observed ZBPs in the tunneling spectra [59–61]. Theoretically, recent works have predicted the emergence of topological states in DNA molecules under a gate field normal to the helix axis [62, 63]. While in proximity to an *s*-wave superconductor, single-stranded DNA (ssDNA) supports a topological nontrivial phase with one pair of MZMs at the ends when the Zeeman field is parallel to the helix axis [64]. However, as ssDNA molecules are unstable and present insulating behavior, the topological superconductivity may be inaccessible experimentally in ssDNA molecules.

In this paper, we study the topological superconductivity of a dsDNA molecule coupled to an *s*-wave superconductor, in the presence of weak spin–orbit coupling (SOC) and a Zeeman field, as illustrated in figure 1. The energy spectra and the differential conductance of this dsDNA-superconductor system are calculated by considering several factors, including the Zeeman field, gate voltage, and Anderson disorder. Our results demonstrate that no topological superconductivity could be observed in the dsDNA-superconductor system when the Zeeman field points along the molecular helix axis (*z* axis in figure 1), which is different from previous studies on an ssDNA-superconductor system which hosts MZMs for parallel Zeeman field. In contrast, the dsDNA-superconductor system host MZMs at the ends when the Zeeman field is perpendicular to the helix axis. This hybrid system exhibits identical topological superconductivity when the Zeeman field points along either the *x* axis or *y* axis. In particular, two topological phase transitions could occur in the dsDNA-superconductor system by tuning the Zeeman field, one from a topological trivial phase to a topological nontrivial phase with one pair of MZMs in small Zeeman field regime and the other from a phase with one pair of MZMs to a phase with two pairs of MZMs by further increasing the Zeeman field. The topological nontrivial phase with one pair of MZMs is more stable than the phase with two pairs of MZMs due to larger gap in the former case. Besides, in the presence of a gate field normal to the helix axis, a topological phase transition from the phase with two pairs of MZMs to the phase with one pair of MZMs could take place by increasing the gate voltage as well. Furthermore, the topological nontrivial phase with one pair of MZMs is robust against Anderson disorder.

## 2. Model and method

The electron transport along two-terminal dsDNA devices on top of  $s$ -wave superconducting substrates, as illustrated in figure 1, will be described by the Hamiltonian  $\mathcal{H} = \mathcal{H}_0 + \mathcal{H}_{\text{el}}$ , where  $\mathcal{H}_0$  and  $\mathcal{H}_{\text{el}}$  represent the dsDNA-superconductor hybrid system and the electrodes including the molecule–electrode couplings, respectively. The Hamiltonian of dsDNA molecules in proximity with the  $s$ -wave superconductor can be written as [64, 65]:

$$\begin{aligned} \mathcal{H}_0 = \sum_{j=1}^2 \left\{ \sum_{n=1}^N (\varepsilon_{jn} - \mu) c_{jn}^\dagger c_{jn} + \sum_{n=1}^{N-1} [it_{\text{so}} c_{jn}^\dagger (\sigma_n^{(j)} + \sigma_{n+1}^{(j)}) c_{j,n+1} + t c_{jn}^\dagger c_{j,n+1} + \text{H.c.}] \right\} \\ + \sum_{n=1}^N (\lambda c_{1n}^\dagger c_{2n} + \text{H.c.}) + \sum_{j=1}^2 \sum_{n=1}^N (B_\alpha c_{jn}^\dagger \sigma_\alpha c_{jn} + \Delta c_{j\uparrow}^\dagger c_{j\downarrow} + \text{H.c.}). \end{aligned} \quad (1)$$

Here, all the terms in the first and second lines are the Hamiltonian of usual two-leg ladder model including the SOC one, with  $c_{jn}^\dagger = (c_{j\uparrow}^\dagger, c_{j\downarrow}^\dagger)$  being the creation operator at site  $\{j, n\}$  of the dsDNA molecule,  $j$  labeling the helical strand,  $n$  the base-pair index, and  $N$  the molecular length.  $\varepsilon_{jn}$  is the on-site energy,  $\mu$  the chemical potential,  $t_{\text{so}}$  the SOC strength, and  $t$  ( $\lambda$ ) the intrachain (interchain) hopping integral. The SOC term is expressed as  $\sigma_{n+1}^{(j)} = (-1)^{j+1} [\sigma_x \sin(n\Delta\phi) - \sigma_y \cos(n\Delta\phi)] \sin\theta + \sigma_z \cos\theta$ , with  $\sigma_{\alpha(\alpha=x,y,z)}$  the Pauli matrices,  $\Delta\phi$  the twist angle, and  $\theta$  the space angle between the helical strand and the  $x$ - $y$  plane [65]. The first term in the third line describes the Zeeman splitting under an external magnetic field whose direction can be tuned toward any coordinate axis, while the second one accounts for the proximity effect induced by the  $s$ -wave superconductor, with  $B_\alpha$  the Zeeman energy and  $\Delta$  the pairing potential.

We consider the dsDNA molecule coupled to left (L) and right (R) normal-metal electrodes at the two ends. Then, the Hamiltonian of these electrodes and their couplings to the dsDNA molecule can be written in momentum space

$$\mathcal{H}_{\text{el}} = \sum_{k,\beta=L,R} [\varepsilon_k a_{\beta k}^\dagger a_{\beta k} + \tau a_{\beta k}^\dagger (c_{1n_\beta} + c_{2n_\beta}) + \text{H.c.}], \quad (2)$$

where  $n_L = 1$ ,  $n_R = N$ ,  $a_{\beta k}^\dagger = (a_{\beta k\uparrow}^\dagger, a_{\beta k\downarrow}^\dagger)$  is the creation operator in the  $\beta$  electrode with momentum  $k$  and energy  $\varepsilon_k$ , and  $\tau$  is the tunneling amplitude between the dsDNA and the electrodes.

The current flowing from the left electrode to the dsDNA can be obtained from the time derivative of the total electron number in the left electrode [66]

$$I = -e \left\langle \frac{d}{dt} \sum_k a_{Lk}^\dagger a_{Lk} \right\rangle. \quad (3)$$

In the spin  $\otimes$  Nambu space constructed by the basis vector  $[c_{1n\uparrow}, c_{1n\downarrow}, c_{1n\downarrow}, c_{1n\uparrow}, c_{2n\uparrow}, c_{2n\downarrow}, c_{2n\downarrow}, c_{2n\uparrow}]^T$ , the current can be calculated by using the Green's function and expressed as [67, 68]

$$I = \frac{e}{h} \int dE \text{Re} \text{Tr}[\boldsymbol{\sigma}(\mathbf{G}^< \boldsymbol{\Sigma}_L^a + \mathbf{G}^r \boldsymbol{\Sigma}_L^<)]. \quad (4)$$

Here,  $\boldsymbol{\sigma} = \text{diag}(1, -1, 1, -1, 1, -1, 1, -1)$  represents the different charge carried by electrons and holes, and the trace is performed over the spin  $\otimes$  Nambu space. The retarded Green's function  $\mathbf{G}^r = [E - \mathbf{H}_0 - \boldsymbol{\Sigma}_L^r - \boldsymbol{\Sigma}_R^r]^{-1}$ , and  $\boldsymbol{\Sigma}_\beta^{r/a}$  is the retarded/advanced self-energy due to the coupling to electrode  $\beta$ . Here, we consider the wide-band limit and the self-energy is taken as  $\boldsymbol{\Sigma}_\beta^r = (\boldsymbol{\Sigma}_\beta^a)^* = -i\Gamma/2$ , with  $\Gamma$  being the coupling strength between the electrodes and the dsDNA. Finally, the lesser Green's function can be obtained from the Keldysh equation

$$\mathbf{G}^< = \mathbf{G}^r \boldsymbol{\Sigma}^< \mathbf{G}^a, \quad (5)$$

where  $\boldsymbol{\Sigma}^< = \boldsymbol{\Sigma}_L^< + \boldsymbol{\Sigma}_R^<$  is the lesser self-energy. Based on the fluctuation–dissipation theorem,  $\boldsymbol{\Sigma}_{L/R}^<$  is written as

$$\boldsymbol{\Sigma}_L^< = \begin{bmatrix} \boldsymbol{\Sigma}_{L0}^< & \boldsymbol{\Sigma}_{L0}^< & 0 & \dots \\ \boldsymbol{\Sigma}_{L0}^< & \boldsymbol{\Sigma}_{L0}^< & 0 & \dots \\ 0 & 0 & 0 & \dots \\ \dots & \dots & \dots & \dots \end{bmatrix}, \quad \boldsymbol{\Sigma}_R^< = \begin{bmatrix} \dots & \dots & \dots & \dots \\ \dots & 0 & 0 & 0 \\ \dots & 0 & \boldsymbol{\Sigma}_{R0}^< & \boldsymbol{\Sigma}_{R0}^< \\ \dots & 0 & \boldsymbol{\Sigma}_{R0}^< & \boldsymbol{\Sigma}_{R0}^< \end{bmatrix}, \quad (6)$$

where  $\Sigma_{\beta 0}^< = i\Gamma \text{diag}[f(E - \mu_{\beta}), f(E + \mu_{\beta}), f(E - \mu_{\beta}), f(E + \mu_{\beta})]$ ,  $\mu_{\beta}$  is the chemical potential in the  $\beta$  electrode, and  $f(E)$  is the Fermi distribution function. The chemical potential is set to  $\mu_L = eV_b/2$  and  $\mu_R = -eV_b/2$ , and the temperature to zero as the temperature is very low in experiments, with  $V_b$  the bias voltage between the left and right electrodes. Then, the differential conductance can be obtained from equation (4) as

$$G = \frac{dI}{dV_b}. \quad (7)$$

### 3. Results and discussion

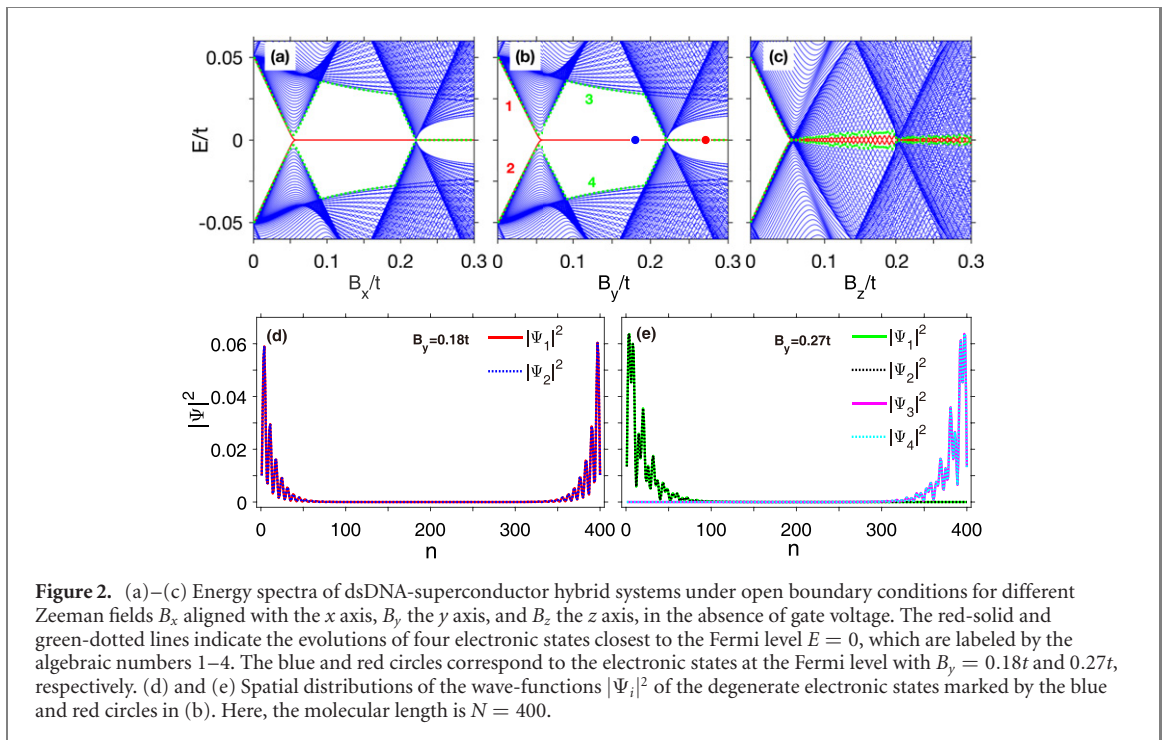
In the numerical calculations, the intrachain hopping integral is taken as the energy unit,  $t = 1$ , and the on-site energy in the first helical-strand as the energy reference point,  $\varepsilon_{1n} = \varepsilon_1 = 0$ . Other model parameters are then taken as  $\varepsilon_{2n} = \varepsilon_2 = 3t$ ,  $t_{so} = 0.1t$ , and  $\lambda = 1.5t$  [65]. The structural parameters are set to  $N = 400$ ,  $\Delta\phi = \pi/5$ , and  $\theta \approx 0.66$ . The coupling strength between the electrodes and the dsDNA is  $\Gamma = 0.05t$ , the pairing potential  $\Delta = 0.05t$ , and the chemical potential  $\mu = 1.4t$  which could be tuned by dual gate electrodes. These parameters will be used throughout the paper, unless stated otherwise.

#### 3.1. Signatures of MZMs in topological superconducting dsDNA devices

We first consider the dsDNA-superconductor hybrid system in the absence of gate voltage and disorder. Figures 2(a), (b) and (c) show the energy spectra under open boundary conditions as functions of the Zeeman energies  $B_x$ ,  $B_y$ , and  $B_z$  along different coordinate axes, respectively. By inspecting figure 2(c), it clearly appears that the energy spectrum is symmetric with respect to the line  $E = 0$  when the Zeeman field points along the  $z$  axis, owing to the electron–hole symmetry in the superconductor. In the absence of Zeeman field, there exists an energy gap with size  $2\Delta$  because of the proximity-induced effect in dsDNA molecules, implying that the dsDNA-superconductor system behaves as a conventional BCS superconductor for  $B_z = 0$ . By increasing  $B_z$ , this energy gap decreases linearly and closes at  $B_z \sim 0.055t$ , with no topological gap for whatever the value of  $B_z$ . This indicates that the dsDNA-superconductor system cannot present topological superconductivity when the Zeeman field is parallel to the helix axis, in sharp contrast to the ssDNA-superconductor system which hosts MZMs for parallel Zeeman field [64]. This may be understood as follows. Since the  $x$  ( $y$ ) component of the SOC of the first helical-strand is opposite to that of the second one due to the  $\pi$  phase difference between the cylindrical coordinates of two pairing nucleobases [65], the effective SOC of the dsDNA molecules should point along the  $z$  axis. As a result, the effective SOC is parallel to the Zeeman field in this situation and thus no topological superconductivity could be detected in the dsDNA-superconductor system when the Zeeman field is aligned with the helix axis [22].

When the Zeeman field points along either the  $x$  axis or the  $y$  axis, the energy spectra are identical to each other (see figures 2(a) and (b)), and below we consider the Zeeman field pointing along the  $y$  axis as an example. One can see from figure 2(b) that the energy spectra are symmetric with respect to the line  $E = 0$ , and the energy gap decreases linearly with  $B_y$  and closes at  $B_y \sim 0.055t$ , which are similar to the case when the Zeeman field points along the  $z$  axis. As a result, the dsDNA-superconductor system does not exhibit topological superconductivity and locates in topological trivial phase for  $B_y < 0.055t$ . Interestingly, different phenomena could be observed in the dsDNA-superconductor system in relatively large Zeeman field regime when the Zeeman field is perpendicular to the helix axis. When the Zeeman field is increased beyond  $B_y \sim 0.055t$ , a topological gap emerges in the energy spectrum, demonstrating a topological phase transition from a topological trivial phase to a topological nontrivial one. In the topological nontrivial regime, the energy levels 1 and 2 become degenerated and are equal to zero (see the solid-red lines in figure 2(b)). These two zero modes are MZMs, which are protected by the topological gap. For further confirmation, figure 2(d) shows the probability distribution  $|\Psi_n|^2$  of energy level  $n$  ( $n = 1, 2$ ) at  $B_y = 0.18t$  (see the blue dot in figure 2(b)), which is obtained by diagonalizing the Hamiltonian of isolated dsDNA-superconductor system (see equation (1)). The probability distributions  $|\Psi_1|^2$  and  $|\Psi_2|^2$  are superimposed with each other, and the electronic states are localized at the ends of the dsDNA molecules, indicating that the dsDNA-superconductor system is a topological nontrivial phase with one pair of MZMs.

Besides, one can see that the band gap closes again at  $B_y \sim 0.222t$  and reopens when the Zeeman field surpasses this critical value. The gap width increases gradually with  $B_y$  when  $B_y > 0.222t$ , but its magnitude is smaller than that in the region  $0.055t \leq B_y \leq 0.222t$ . Similarly, the energy levels 3 and 4 become degenerated and are equal to zero (see the green-dotted lines in figure 2(b)), just the same as the energy levels 1 and 2. In a word, the energy levels 1–4 are degenerated in larger Zeeman field region. The probability distributions of the electronic states 1–4 at  $B_y = 0.27t$  (see the red dot in figure 2(b)) are shown in figure 2(e). It clearly appears that these four zero modes are localized at the ends of the dsDNA



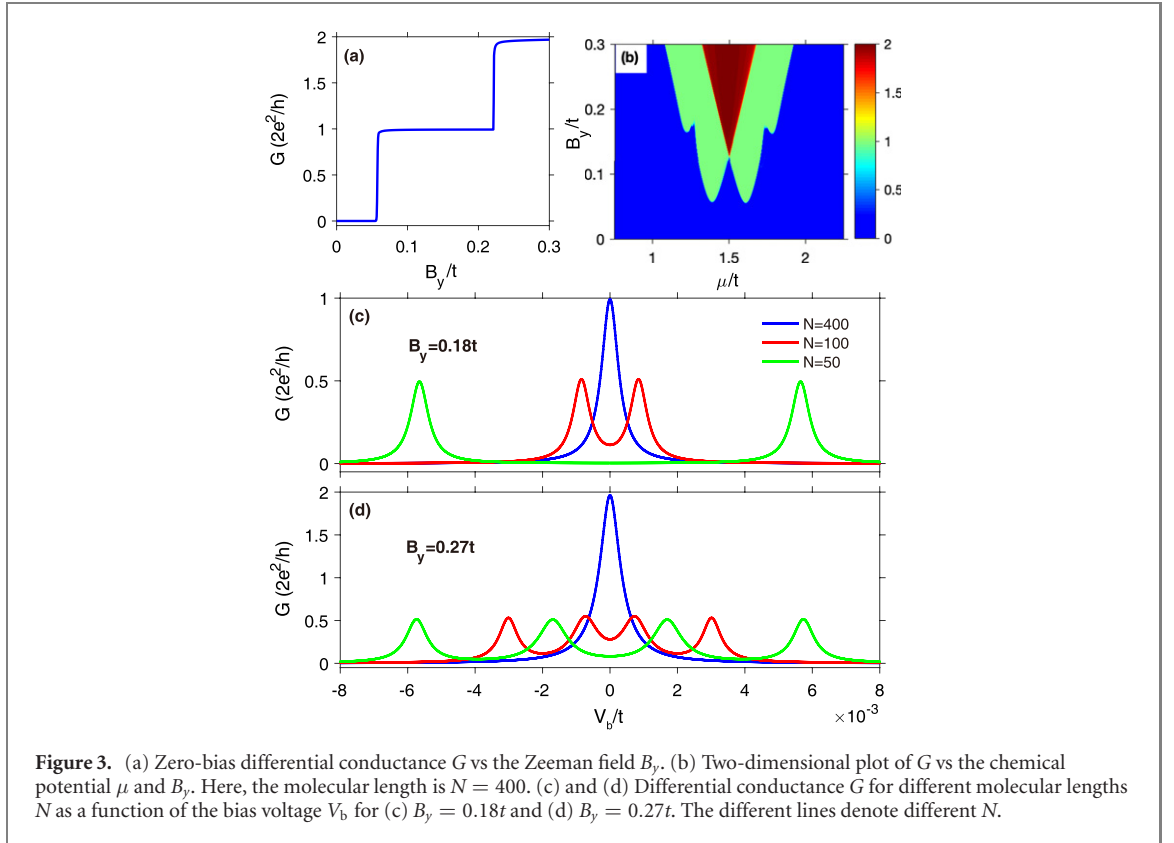
molecules, implying that these four zero modes are MZMs as well. Therefore, this region is also a topological nontrivial phase, but hosts two pairs of MZMs at the ends of the dsDNA molecules. Notice that Ray *et al* numerically computed both energy spectrum and conductance of a quasi-1D Rashba nanowire which is composed of three weakly coupled 1D chains [69], finding that this quasi-1D nanowire hosts three pairs of MZMs. It would be reasonable that dsDNA, which consists of two helical chains, hosts two pairs of MZMs under certain parameters.

When  $\Delta = 0.05t$ , the critical Zeeman energy to observe the phase with one pair of MZMs in dsDNA is about  $0.055t$ , which is smaller than the critical Zeeman energy in ssDNA [64]. In particular, further studies indicate that the critical Zeeman energy for this phase decreases almost linearly with decreasing  $\Delta$ . In other words, the critical magnetic field to observe one pair of MZMs decreases almost linearly with decreasing  $\Delta$ . For example, the critical magnetic field for one pair of MZMs is about 14 T when  $\Delta = 1$  meV, which is accessible in experiments. Although the critical Zeeman field for the phase with two pairs of MZMs decreases slightly with decreasing  $\Delta$ , it could be dramatically reduced by tuning  $\mu$ . In other words, the critical magnetic field to observe two pairs of MZMs could be reduced by tuning  $\mu$ .

In particular, in recent, Ising superconductivity is experimentally realized and it has the strong magnetic anisotropy [70–72]. Owing to the strong pinning of electron spins to the out-of-plane direction by Ising SOC, external in-plane magnetic field is much less effective in aligning electron spins. Therefore, Ising SOC significantly increases the in-plane upper critical magnetic field, which can reach 52 T at 1.5 K [71]. Therefore, topological superconducting phase may be realized experimentally in dsDNA by using Ising superconductors which have superconductivity under high magnetic fields.

To further understand the topology of the dsDNA-superconductor system, we consider a two-terminal dsDNA device (see figure 1) and calculate its differential conductance. For the left and right normal-metal electrodes, the symmetric condition is taken into account and the linewidth function is fixed to  $\Gamma_L = \Gamma_R = 0.05t$ . Figure 3(a) shows the differential conductance  $G$  at zero bias voltage as a function of the Zeeman energy  $B_y$ . One can identify two distinct plateaus in the curve  $G - B_y$ . Here, a conductance plateau always corresponds to a new phase or the emergence of a novel phenomenon. As compared with the energy spectrum (see figure 2(b)), the low conductance plateau corresponds to the topological nontrivial phase with one pair of MZMs and the high conductance plateau to the phase with two pairs of MZMs. The low conductance plateau is exactly equal to  $2e^2/h$ , while the high one is slightly less than  $4e^2/h$ , which can be understood as follows. Since the gap width of the topological nontrivial phase with one pair of MZMs is larger than that with two pairs of MZMs (see figures 2(a) and (b)), the MZMs in the phase with two pairs of MZMs tends to couple with each other and results in non-integer differential conductance which is slightly less than  $4e^2/h$ .

Figure 3(b) plots the contour map of the zero-bias differential conductance as functions of the Zeeman energy  $B_y$  and the chemical potential  $\mu$ . The blue region is the topological trivial phase with no MZM in



this area, whereas the green and dark red regions are the topological nontrivial phases that host one and two pairs of MZMs, respectively. Moreover, the conductance is symmetrical with respect to the chemical potential  $\mu = 1.5t$ , and the minimum Zeeman energy for two pairs of MZMs is about  $0.126t$ . Therefore, the MZM and the topological phase transition of the dsDNA-superconductor system can be realized by adjusting the Zeeman energy and the chemical potential.

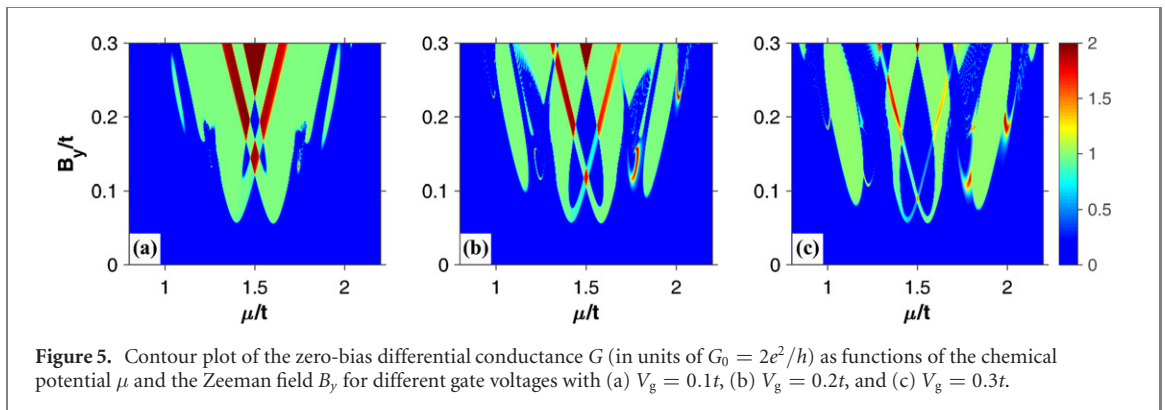
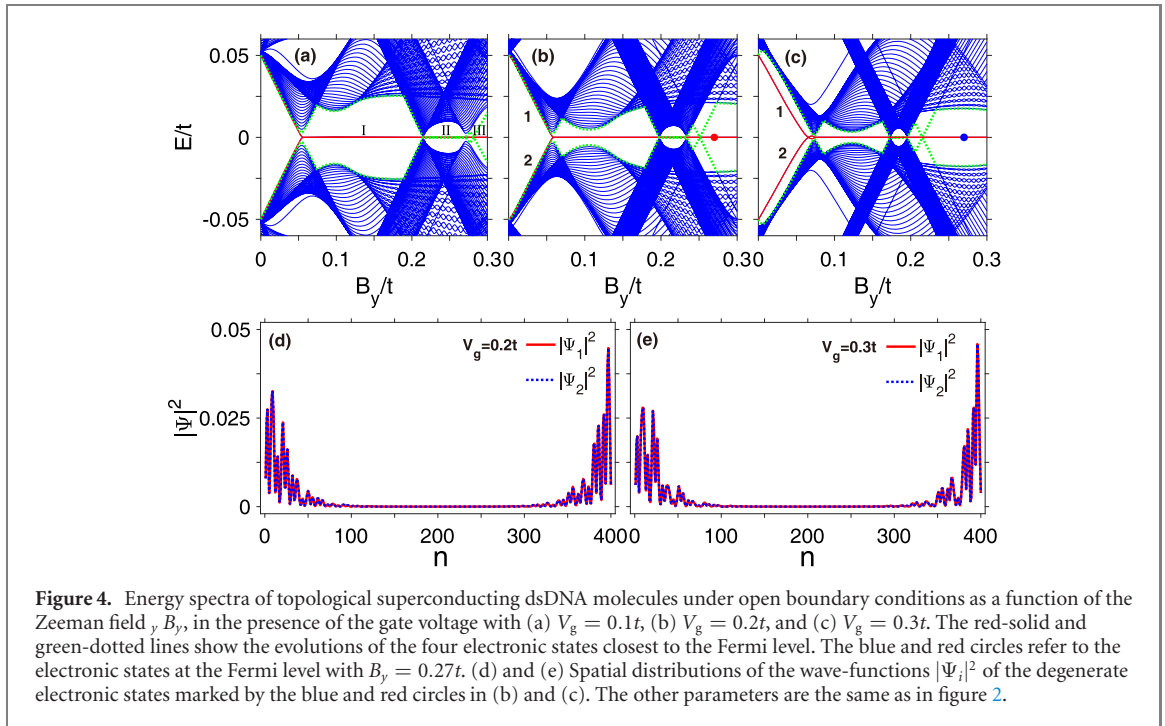
To further demonstrate the MZMs in the dsDNA-superconductor system, figures 3(c) and (d) display the differential conductance as a function of the bias voltage  $V_b$  by considering various molecular lengths  $N$  with the Zeeman field  $B_y = 0.18t$  and  $B_y = 0.27t$ , respectively, which correspond to the topological nontrivial phase with one and two pairs of MZMs. One can see that when the molecular length is sufficiently large, e.g.,  $N = 400$  (see the blue line in figure 3(c)), the differential conductance  $G$  displays a single-peak structure, with the peak locating at zero bias voltage and its value being  $2e^2/h$  exactly, because the two MZMs are far from each other and the coupling between them is negligible when the molecular length is sufficiently large. This single-peak structure can also be observed for  $B_y = 0.27t$  (see the blue line in figure 3(d)). However, the peak value is slightly less than  $4e^2/h$  due to the coupling between the two pairs of MZMs. When the molecular length becomes shorter, the single-peak structure disappears, and the zero-bias peak splits into two peaks for  $B_y = 0.18t$  (see the red and green lines in figure 3(c)) and into four peaks for  $B_y = 0.27t$  (see the red and green lines in figure 3(d)), with the peak value approaching half conductance quantum  $2e^2/h$ . Besides, one can see that the peaks will be farther away from each other when the molecular length becomes shorter.

### 3.2. Gating effect on Majorana zero modes in topological superconducting dsDNA devices

Then we study the effect of a gate voltage on the topological nontrivial phase of the dsDNA-superconductor system. In the presence of an external electric field  $E_g$  which is normal to the helix axis, the on-site energy takes the form [62, 63, 73]

$$\varepsilon_{jn} = \varepsilon_j - (-1)^j eV_g \cos(n\Delta\phi). \quad (8)$$

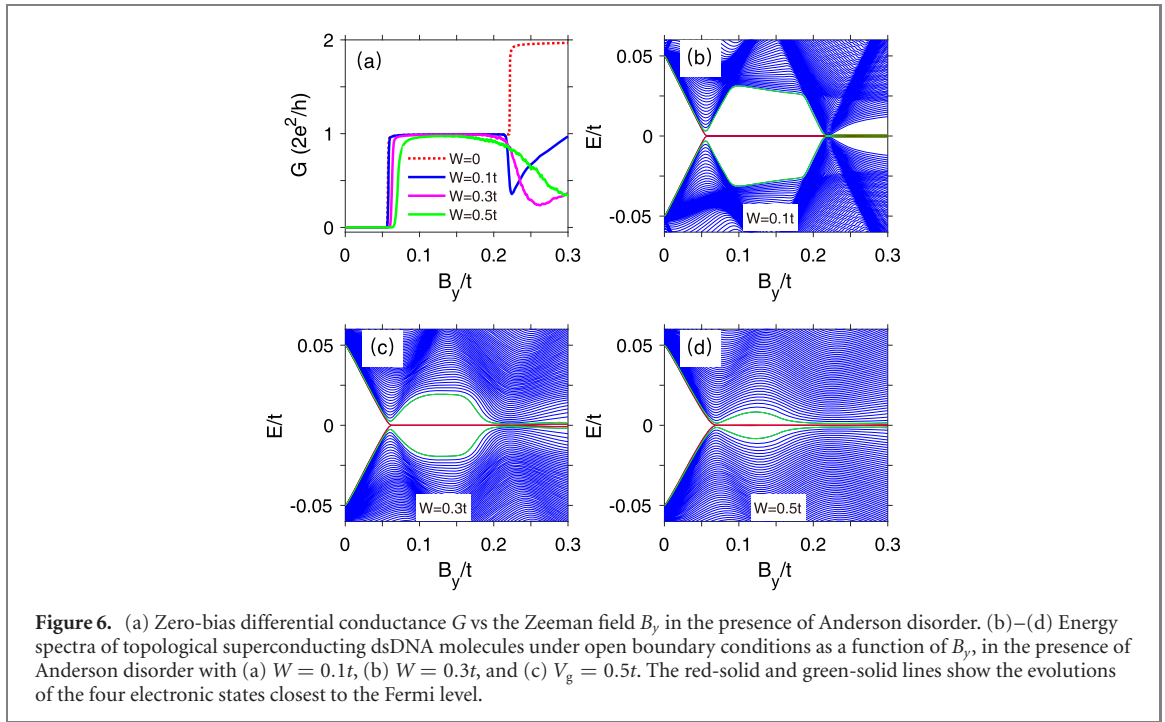
Here,  $2V_g = 2E_g R$  is the gate voltage drop along the cross section of the dsDNA molecule and  $R$  is the molecular radius. Figures 4(a), (b) and (c) show the energy spectra of the dsDNA-superconductor system for different gate voltages  $V_g$  as a function of the Zeeman energy  $B_y$ . In the presence of the gate voltage, more phases will appear in the dsDNA-superconductor system, which are labeled by I, II, and III, as illustrated in figure 4(a). Phase I and phase II are the same as the two topological nontrivial phases in the absence of the gate voltage (see figure 2(b)), which host one and two pairs of MZMs, respectively. Phase III



is a novel phase induced by the gate voltage, where two zero modes emerge in this regime. To investigate these two zero modes, figures 4(d) and (e) display the probability distribution of these zero modes for  $V_g = 0.2t$  (red dot in figure 4(b)) and  $V_g = 0.3t$  (blue dot in figure 4(e)), respectively. Although the symmetry of the probability distribution is destroyed by the gate voltage, these zero modes are still localized at the ends of the dsDNA molecule for whatever the value of  $V_g$ , and the corresponding conductance is exactly equal to  $2e^2/h$  (see figure 5), indicating that phase III is also a topological nontrivial phase which hosts one pair of MZMs. Therefore, in the presence of a gate voltage, the topological phase transition could occur in the dsDNA-superconductor system and the topological nontrivial phase with two pairs of MZMs can transform into the phase with one pair of MZMs.

Besides, one can see from figures 4(a), (b) and (c) that the gap width of phase I and phase II is declined by increasing the gate voltage, where the gap width of both phases is very small when the gate voltage is taken as  $V_g = 0.3t$ . In contrast, the gap width is relatively large for phase III, implying that the MZMs of phase III are more stable than those of phases I and II. In addition, phases I and II move toward small Zeeman fields and their region decreases with increasing the gate voltage, whereas the region of phase III increases with the gate voltage. This indicates that one pair of stable MZMs can be found in the dsDNA-superconductor system within a wider Zeeman field for larger gate voltage.

Figure 5 shows the corresponding zero-bias differential conductance  $G$  as functions of the Zeeman energy  $B_y$  and the chemical potential  $\mu$  for different gate voltages  $V_g$ . It clearly appears that a part of the region with differential conductance being about  $4e^2/h$  in the absence of the gate voltage will be changed into the region with conductance being  $2e^2/h$ . This further demonstrates a topological phase transition in the dsDNA-superconductor system induced by the gate voltage, where the topological nontrivial phase with



two pairs of MZMs can transform into the phase with one pair of MZMs when a gate field is applied perpendicularly to the helix axis. The region with conductance  $2e^2/h$  becomes wider when the gate voltage is increased, and most of the region with two pairs of MZMs will transform into the region with one pair of MZMs for  $V_g = 0.3t$ . Although the phase with two pairs of MZMs is destroyed by the gate voltage, the phase with one pair of stable MZMs exists over a wider region.

### 3.3. Disorder effect on Majorana zero modes in topological superconducting dsDNA devices

In real experiments, disorder exists inevitably in the system and usually plays a significant role in the transport property. Here, we consider the most disordered case that the on-site energy  $\varepsilon_{jn}$  is distributed randomly and uniformly within the range  $[\varepsilon_j - W/2, \varepsilon_j + W/2]$ , with  $W$  the disorder strength. Figure 6(a) shows the zero-bias differential conductance for several disorder strengths  $W$  as a function of the Zeeman energy  $B_y$ , and figures 6(b), (c) and (d) plot the corresponding energy spectra. In all of these calculations, the results are averaged over 500 disorder configurations. It is clear that the low conductance plateau is robust against Anderson disorder, whereas the high conductance plateau is fragile upon weak disorder. One can see from figures 6(b), (c) and (d) that the gap width corresponding to the topological nontrivial phase with two pairs of MZMs decreases quickly with increasing  $W$ , while the gap width corresponding to the topological nontrivial phase with one pair of MZMs remains significant for relatively large  $W$ . Since the topological nontrivial phase is protected by the gap, the topological nontrivial phase with two pairs of MZMs disappears while the topological nontrivial phase with one pair of MZMs still exists. As the disorder strength is increased up to  $W = 0.5t$ , the topological gap corresponding to the topological nontrivial phase with one pair of MZMs becomes smaller and thus the width of the corresponding conductance plateau is reduced.

## 4. Summary

In summary, we have investigated the energy spectrum and differential conductance of a dsDNA-superconductor system using the tight-binding method. Our simulations indicate that two kinds of topological nontrivial phases are present in the dsDNA-superconductor system in the presence of a Zeeman field pointing along either the  $x$  axis or the  $y$  axis. One of the topological nontrivial phases hosts one pair of MZMs and the other hosts two pairs of MZMs. The topological nontrivial phase with one pair of MZMs is more stable due to its larger topological gap. And the topological nontrivial phase with two pairs of MZMs can transform into a topological nontrivial phase with one pair of MZMs when one applies a gate voltage. Additionally, the topological nontrivial phase with one pair of MZMs is robust against weak disorder.

## Acknowledgments

We thank Chui-Zhen Chen for useful discussions. This work is supported by National Natural Science Foundation of China (Grant Nos. 11874428 and 11921005), Hunan Provincial Natural Science Foundation of China (Grant No. 2020JJ4240), and National Key Research and Development Program of China (Grant Nos. 2017YFA0303301 and 2018YFB0704000).

## Data availability statement

The data that support the findings of this study are available upon reasonable request from the authors.

## References

- [1] Kitaev A Y 2001 *Phys.-Usp.* **44** 131
- [2] Fu L and Kane C L 2008 *Phys. Rev. Lett.* **100** 096407
- [3] Law K T, Lee P A and Ng T K 2009 *Phys. Rev. Lett.* **103** 237001
- [4] Flensberg K 2010 *Phys. Rev. B* **82** 180516(R)
- [5] Sau J D, Tewari S, Lutchyn R M, Stanescu T D and Das Sarma S 2010 *Phys. Rev. B* **82** 214509
- [6] Qi X-L and Zhang S-C 2011 *Rev. Mod. Phys.* **83** 1057
- [7] Alicea J 2012 *Rep. Prog. Phys.* **75** 076501
- [8] Deng M T, Yu C L, Huang G Y, Larsson M, Caroff P and Xu H Q 2012 *Nano Lett.* **12** 6414
- [9] Das A, Ronen Y, Most Y, Oreg Y, Heiblum M and Shtrikman H 2012 *Nat. Phys.* **8** 887
- [10] Churchill H O H, Fatemi V, Grove-Rasmussen K, Deng M T, Caroff P, Xu H Q and Marcus C M 2013 *Phys. Rev. B* **87** 241401(R)
- [11] Finck A D K, Van Harlingen D J, Mohseni P K, Jung K and Li X 2013 *Phys. Rev. Lett.* **110** 126406
- [12] Sun H-H *et al* 2016 *Phys. Rev. Lett.* **116** 257003
- [13] Cheng S-G, Liu J, Liu H, Jiang H, Sun Q-F and Xie X C 2020 *Phys. Rev. B* **101** 165420
- [14] Wang X-Q, Zhang S-F, Han Y, Yi G-Y and Gong W-J 2019 *Phys. Rev. B* **99** 195424
- [15] Sau J D, Lutchyn R M, Tewari S and Das Sarma S 2010 *Phys. Rev. Lett.* **104** 040502
- [16] Alicea J, Oreg Y, Refael G, von Oppen F and Fisher M P A 2011 *Nat. Phys.* **7** 412
- [17] Sarma S D, Freedman M and Nayak C 2015 *npj Quantum Inf.* **1** 15001
- [18] Vijay S and Fu L 2016 *Phys. Rev. B* **94** 235446
- [19] Karzig T *et al* 2017 *Phys. Rev. B* **95** 235305
- [20] Chen C-Z, Xie Y-M, Liu J, Lee P A and Law K T 2018 *Phys. Rev. B* **97** 104504
- [21] Lutchyn R M, Sau J D and Das Sarma S 2010 *Phys. Rev. Lett.* **105** 077001
- [22] Oreg Y, Refael G and von Oppen F 2010 *Phys. Rev. Lett.* **105** 177002
- [23] Stanescu T D, Lutchyn R M and Das Sarma S 2011 *Phys. Rev. B* **84** 144522
- [24] Mourik V, Zuo K, Frolov S M, Plissard S R, Bakkers E P A M and Kouwenhoven L P 2012 *Science* **336** 1003
- [25] Albrecht S M, Higginbotham A P, Madsen M, Kuemmeth F, Jespersen T S, Nygård J, Krogstrup P and Marcus C M 2016 *Nature* **531** 206
- [26] Deng M T, Vaitiekėnas S, Hansen E B, Danon J, Leijnse M, Flensberg K, Nygård J, Krogstrup P and Marcus C M 2014 *Science* **354** 1557
- [27] Liu J, Song J, Sun Q-F and Xie X C 2017 *Phys. Rev. B* **96** 195307
- [28] Nadj-Perge S, Drozdov I K, Li J, Chen H, Jeon S, Seo J, MacDonald A H, Bernevig B A and Yazdani A 2014 *Science* **346** 602
- [29] Li J, Chen H, Drozdov I K, Yazdani A, Bernevig B A and MacDonald A H 2014 *Phys. Rev. B* **90** 235433
- [30] Ruby M, Pientka F, Peng Y, von Oppen F, Heinrich B W and Franke K J 2015 *Phys. Rev. Lett.* **115** 197204
- [31] Jeon S, Xie Y, Li J, Wang Z, Bernevig B A and Yazdani A 2017 *Science* **358** 772
- [32] Kim H, Palacio-Morales A, Posske T, Rózsa L, Palotás K, Szunyogh L, Thorwart M and Wiesendanger R 2018 *Sci. Adv.* **4** eaar5251
- [33] Hell M, Leijnse M and Flensberg K 2017 *Phys. Rev. Lett.* **118** 107701
- [34] Pientka F, Keselman A, Berg E, Yacoby A, Stern A and Halperin B I 2017 *Phys. Rev. X* **7** 021032
- [35] Fornieri A *et al* 2019 *Nature* **569** 89
- [36] Ren H *et al* 2019 *Nature* **569** 93
- [37] Wu B-H, Hassan S A, Xu X-F, Wang C-R, Gong W-J and Cao J-C 2020 *Phys. Rev. B* **102** 085414
- [38] Laeven T, Nijholt B, Wimmer M and Akhmerov A R 2020 *Phys. Rev. Lett.* **125** 086802
- [39] Zhang P *et al* 2018 *Science* **360** 182
- [40] Wang D *et al* 2018 *Science* **362** 333
- [41] Zhang R-X, Cole W S and Das Sarma S 2019 *Phys. Rev. Lett.* **122** 187001
- [42] Wang Z, Rodriguez J O, Jiao L, Howard S, Graham M, Gu G D, Hughes T L, Morr D K and Madhavan V 2020 *Science* **367** 104
- [43] Zhu S *et al* 2020 *Science* **367** 189
- [44] Liu J, Potter A C, Law K T and Lee P A 2012 *Phys. Rev. Lett.* **109** 267002
- [45] Bagrets D and Altland A 2012 *Phys. Rev. Lett.* **109** 227005
- [46] Pikulin D I, Dahlhaus J P, Wimmer M, Schomerus H and Beenakker C W J 2012 *New J. Phys.* **14** 125011
- [47] Lee E J H, Jiang X, Aguado R, Katsaros G, Lieber C M and De Franceschi S 2012 *Phys. Rev. Lett.* **109** 186802
- [48] Lee E J H, Jiang X, Houzet M, Aguado R, Lieber C M, De Franceschi S and Franceschi S D 2014 *Nat. Nanotechnol.* **9** 79
- [49] Zhang F, Jiang S, Wu S, Li Y, Mao C, Liu Y and Yan H 2015 *Nat. Nanotechnol.* **10** 779
- [50] Seeman N C and Sleiman H F 2018 *Nat. Rev. Mater.* **3** 17068
- [51] Woods D, Doty D, Myhrvold C, Hui J, Zhou F, Yin P and Winfree E 2019 *Nature* **567** 366
- [52] Yoo K-H, Ha D H, Lee J-O, Park J W, Kim J, Kim J J, Lee H-Y, Kawai T and Choi H Y 2001 *Phys. Rev. Lett.* **87** 198102
- [53] Roy S *et al* 2008 *Nano Lett.* **8** 26
- [54] Xiang L, Palma J L, Li Y, Mujica V, Ratner M A and Tao N 2017 *Nat. Commun.* **8** 14471

- [55] Göhler B, Hamelbeck V, Markus T Z, Kettner M, Hanne G F, Vager Z, Naaman R and Zacharias H 2011 *Science* **331** 894
- [56] Zwang T J, Hürlimann S, Hill M G and Barton J K 2016 *J. Am. Chem. Soc.* **138** 15551
- [57] Naaman R, Paltiel Y and Waldeck D H 2019 *Nat. Rev. Chem.* **3** 250
- [58] Kasumov A Y, Kociak M, Guéron S, Reulet B, Volkov V T, Klinov D V and Bouchiat H 2001 *Science* **291** 280
- [59] Alpern H, Katzir E, Yochelis S, Katz N, Paltiel Y and Millo O 2016 *New J. Phys.* **18** 113048
- [60] Shapira T, Alpern H, Yochelis S, Lee T-K, Kaun C-C, Paltiel Y, Koren G and Millo O 2018 *Phys. Rev. B* **98** 214513
- [61] Alpern H *et al* 2019 *Nano Lett.* **19** 5167
- [62] Guo A-M and Sun Q-F 2017 *Phys. Rev. B* **95** 155411
- [63] Guo A-M, Hu P-J, Gao X-H, Fang T-F and Sun Q-F 2020 *Phys. Rev. B* **102** 155402
- [64] Tang H-Z, Sun Q-F, Liu J-J and Zhang Y-T 2019 *Phys. Rev. B* **99** 235427
- [65] Guo A-M and Sun Q-F 2012 *Phys. Rev. Lett.* **108** 218102
- [66] Jauho A-P, Wingreen N S and Meir Y 1994 *Phys. Rev. B* **50** 5528
- [67] Sun Q-F and Xie X C 2009 *J. Phys.: Condens. Matter.* **21** 344204
- [68] Wu B-H and Cao J-C 2012 *Phys. Rev. B* **85** 085415
- [69] Ray A B, Sau J D and Mandal I 2021 arXiv:1907.10626v2
- [70] Lu J M *et al* 2015 *Science* **350** 6266
- [71] Saito Y *et al* 2016 *Nat. Phys.* **12** 144–9
- [72] Xi X *et al* 2016 *Nat. Phys.* **12** 139–43
- [73] Guo A-M and Sun Q-F 2012 *Phys. Rev. B* **86** 035424